Short-term phytotoxicity in Brassica napus (L.) in response to pre-emergently applied metazachlor: A microcosm study

Article *in* Environmental Toxicology and Chemistry · June 2016

DOI: 10.1002/etc.3538

CITATIONS
20

READS
126

5 authors, including:

Hanne Vercampt
Hasselt University
11 PUBLICATIONS **355** CITATIONS
SEE PROFILE

Lyubka Koleva
Agricultural University Plovdiv
40 PUBLICATIONS **742** CITATIONS
SEE PROFILE

Andon Vassilev
Agricultural University Plovdiv
95 PUBLICATIONS **3,103** CITATIONS
SEE PROFILE

Jaco Vangronsveld
Hasselt University
770 PUBLICATIONS **44,100** CITATIONS
SEE PROFILE

SETAC PRESS

Environmental Toxicology and Chemistry, Vol. 9999, No. 9999, pp. 1–12, 2016

Printed in the USA

Environmental Chemistry

SHORT-TERM PHYTOTOXICITY IN *BRASSICA NAPUS* (L.) IN RESPONSE TO PRE-EMERGENTLY APPLIED METAZACHLOR: A MICROCOSM STUDY

Hanne Vercampt,† Lyubka Koleva,‡ Andon Vassilev,‡ Jaco Vangronsveld,† and Ann Cuypers*†
†Centre for Environmental Sciences, Hasselt University, Diepenbeek, Belgium
‡Department of Plant Physiology and Biochemistry, Agricultural University of Plovdiv, Plovdiv, Bulgaria

(Submitted 16 February 2016; Returned for Revision 23 March 2016; Accepted 24 June 2016)

Abstract: In accordance with realistic application approaches, a short-term 1-factorial experiment was set up to investigate the phytotoxic impact of pre-emergent application of the chloroacetamide herbicide metazachlor on *Brassica napus*. In addition to morphological parameters, the underlying processes that ultimately determine the extent of herbicide-induced phytotoxicity (i.e., herbicide metabolization and cellular antioxidant defense) were examined. The present study demonstrated that metazachlor provoked fasciation of the leaves closely after emergence, which might be linked to its mode of action whereby cell division is impaired through the inhibition of very long chain fatty acid synthesis. The increased activities of antioxidative enzymes and metabolites in leaf tissue indicated the presence of reactive oxygen species under the influence of metazachlor. This resulted in oxidative damage in the form of membrane lipid peroxidation. Simultaneously, the increased activity of glutathione *S*-transferase and the shift in glutathione redox state suggested activation of the detoxification metabolism. This occurred, however, at the expense of growth, with a temporary reduction in plant height and weight after application. The results indicated that metazachlor disappeared within 3 mo to 4 mo after application, which resulted in the recovery of the crop. In conclusion, metazachlor induces phytotoxicity in the short term, either directly through its mode of action or indirectly through the induction of oxidative stress, which resulted in a temporary reduction in growth. *Environ Toxicol Chem* 2016;9999:1–12. © 2016 SETAC

Keywords: *Brassica napus* Metazachlor Phytotoxicity Stress response Toxic effect

INTRODUCTION

Metazachlor is a pre-emergently used herbicide in the cultivation of oilseed crop, *Brassica napus*, to chemically prevent the settling and growth of broadleaved weeds and annual grasses. As a chloroacetamide, metazachlor is known for inhibiting lipid biosynthesis and hence the formation of very long chain fatty acids [1]. Like most herbicides, metazachlor can affect other nontarget species via soil infiltration, drainage, and runoff [2,3]. Even before it enters the ecosystem, the herbicidal compound can potentially affect the cultivated crop. This can subsequently result in reductions in yield [4], morphological aberrations [5], induction of oxidative stress [6], increased lipid peroxidation of membranes [7], and decreased chlorophyll content [8]. Results derived from field experiments are often subject to large variations between plots from a range of factors, leading to a lack of statistical support. This is a result of the fact that field experiments cannot exclude the complex interaction of external factors, such as direction and rate of drainage, the presence of herbivores (e.g., snails), and heterogeneity of the soil. The present microcosm study aimed to exclude these side effects by the use of a 1-factorial experimental design.

The occurrence and extent of phytotoxicity of metazachlor in *B. napus* are determined either by the crop's capacity to detoxify the herbicide or its capacity to cope with metazachlor-induced oxidative stress. The detoxification metabolism of a crop plays an important role in its tolerance against herbicides, with a significant role for glutathione *S*-transferase (GST) [9,10]. Once herbicidal compounds are present in the cell cytoplasm, the structure and reactivity of the compound will be modified by cytochrome P450 proteins in the first phase of detoxification. In the second phase, the modified herbicidal compound is conjugated with glutathione (GSH) by the action of GSTs. In the third phase of herbicide detoxification, GSH will function as a tag for the compartmentalization of the herbicidal compound into either the vacuole or the cell membrane. Herbicidal compounds are known to induce the activity of GST in most crops species [6,11,12]. Based on their sequence identity, gene organization, and active site residues, plant GST's can be divided into 5 classes; tau, phi, theta, zeta, and lambda [13]. Tau and phi class GSTs are plant-specific and do not occur in mammalian species like all other plant GST classes. Glutathione *S*-transferase isoenzymes that belong to the same class have a 40% to 60% identity in their primary structure. Structurally, GSTs are composed of 2 subunits that can be either identical (homodimeric) or distinct (heterodimeric). Each subunit contains a kinetically independent active site with distinct domains for the GSH (G site) and the electrophilic (H site) substrates. With each subunit encoded by a separate gene, plants contain complex multigene families of GSTs. Hence, the various subunits may be able to dimerize in many permutations, producing multiple homodimeric and heterodimeric GST isoenzymes [14]. The GST isoenzymes involved in xenobiotic metabolism are subjected to discrete regulation, showing distinct but overlapping substrate specificities. From complementation studies, it is likely that quite dissimilar GSTs share similar functions [15]. Despite the association between GSTs and plant stress responses, it remains unclear whether different GST classes are substrate-specific. The inducibility of phi and tau class GSTs after plant exposure to either biotic or abiotic stresses is a characteristic feature of these genes [16]. Several tau class GSTs are known to be strongly induced during cell division [16]. Phi class GSTs have been shown to be

This article includes online-only Supplemental Data.
* Address correspondence to ann.cuypers@uhasselt.be
Published online 27 June 2016 in Wiley Online Library (wileyonlinelibrary.com).
DOI: 10.1002/etc.3538

highly reactive toward chloroacetamide and thiocarbamate herbicides [11,17].

Initially after herbicide application, when detoxification is either activated or at its full turnover, the nondetoxified fraction of cytosolic herbicidal compounds can indirectly cause oxidative damage at different cellular levels by the induction of oxidative stress. Herbicide-induced oxidative stress has been described in crops [18,19] and for chloroacetamides, such as alachlor and metolachlor, in particular [20,21]. Herbicides from different classes of mode of action can negatively affect crop morphology [22] and physiology, ranging from destabilization of cellular membranes [23] to pigment profiles [24]. However, the underlying mechanisms of phytotoxicity are not well addressed in the literature. Because of the relatively short degradation rate of metazachlor, which ranges between 3 mo and 4 mo, it was important to monitor metazachlor-induced phytotoxicity closely after application in the present short-term microcosm study. A 1-factorial microcosm experiment was set up to monitor 1) growth, development, and herbicide uptake of the crop *B. napus* for 9 wk after treatment with metazachlor and 2) cellular structure, such as membrane integrity, pigment, and nutrient content, and cell functioning, such as herbicide detoxification and the antioxidant defense mechanism, of *B. napus* within 2 wk and 4 wk after pre-emergent application of metazachlor.

MATERIALS AND METHODS

Experimental design and methodology

Three days before sowing, *B. napus* (cultivar Remy) seeds were surface-sterilized; seeds were washed in a 0.1% sodium hypochlorite solution for 2 min, subsequently rinsed thoroughly with deionized water for 20 min, and then stored in a closed Petri dish on moistened filter paper. After being incubated in the dark at 4 °C for 2 nights, seeds were separately sown in microcosms on 1.3 kg sandy soil at approximately 1-cm depth. Six seeds were sown in each microcosm. The day after sowing, 10 mL of metazachlor solution was applied to the soil surface in the following concentrations: 0 mM, 0.2 mM, and 0.4 mM metazachlor, which corresponded with 0 mg, 0.5 mg, and 1 mg active ingredient per microcosm. Every 2 d, 10 mL to 50 mL of one-half Hoagland nutrient solution was supplied. Plants were grown in a growth chamber under controlled environmental conditions set at a 12-h photoperiod, 65% relative humidity, and day/night temperatures of 22 °C and 18 °C, respectively. A combination of blue, red, and far-red light-emitting diode modules simulated the photosynthetic active radiation of 200 μmol/m^2 of sunlight. Germination was determined by counting the percentage of seeds emerged within 7 d after metazachlor application. Thereafter, the number of plants was reduced to 1 plant per microcosm. Growth was monitored daily for 7 wk by determining the growth stage of each individual plant according to Lancashire et al. [25]. Metazachlor uptake into the aboveground plant parts was monitored 14 d, 28 d, and 42 d after treatment. Leaf tissue for biochemical analyses was collected 14 d and 28 d after treatment, snap frozen in liquid nitrogen, and subsequently stored at –70 °C. During sampling, weight, root length, and shoot length were measured. In addition to these time points, fresh weight was recorded at 9 wk after treatment (63 d after treatment).

Lipid peroxidation

Lipid peroxidation of cell membranes was determined by the measurement of thiobarbituric acid reactive metabolites [26]. Fresh leaf tissue (100 mg) was homogenized in 0.1% trichloroacetic acid. After 30 min of incubation with 0.5% thiobarbituric acid in 20% trichloroacetic acid at 95 °C, the extract was cooled for 5 min on ice (4 °C) and subsequently centrifuged for 10 min at 20 000 *g* (4 °C). The absorbance of the supernatant was measured at 532 nm and corrected for unspecific binding at 600 nm.

Pigment profile

Chlorophyll *a*, chlorophyll *b*, and carotenoid concentrations were determined according to Lichtenthaler et al. [27]. Fresh leaf material (100 mg) was homogenized in 80% acetone in cooled mortars, in darkness. After centrifugation (9000 *g*, 5 min), the volume of the supernatant was determined and subsequently 10 times diluted in 80% acetone. The leaf extract was measured spectrophotometrically at 663 nm, 646 nm, and 470 nm; and subsequently the pigment profile was calculated.

Potassium leakage

Potassium (K) leakage was monitored as a measure for cell membrane stability. Leaves were cut from plants before the surface was washed with Milli-Q water, dried, and subsequently cut into 2 halves, thereby removing the main leaf nerve. After weighing each half of the leaf, 1 part was incubated in 10 mL of Milli-Q water at 4 °C for 3 h and the other part was incubated in 10 mL of Milli-Q water at 95 °C for 3 h. The concentration of K was determined in both extracts by inductively coupled plasma–optical emission spectroscopy (ICP-OES) and represented the extracellular and the total concentrations of K present in the leaf, respectively.

Hydrogen peroxide quantification

The presence of hydrogen peroxide (H_2O_2) in the first leaf pair was determined by qualitative 3,3′-diaminobenzidine staining [28]. Because 3,3′-diaminobenzidine precipitates as a brown complex after being oxidized by H_2O_2, the latter could be located visually. Leaves were carefully cut at their base, put in the dark, and immediately vacuum-infiltrated with 3,3′-diaminobenzidine in 10 mM disodium phosphate buffer (pH 3) for 5 min. Subsequently, samples were shaken for 4 h at 80 rpm in dark conditions. After bleaching for 15 min in ethanol:acetic acid:glycerol (3:1:1) at 95 °C, leaves were stored in acetic acid (20%) at 4 °C before being monitored. The following day, detailed close-up pictures were taken from each separate leaf using a binocular microscope, a digital camera, and BTV-pro software (Bensoftware).

Total antioxidant capacity

The ferric reducing antioxidant capacity assay was used to determine the capacity of lipophilic and hydrophilic antioxidant fractions [29]. Fresh leaf tissue (100 mg) was homogenized in 0.01 N sodium–ethylenediamine tetraacetic acid (Na-EDTA). After centrifugation (30 min, 15 000 *g*, 4 °C), the hydrophilic fraction was located in the supernatant. The lipophilic fraction, which was located in the pellet, was further extracted in 80% acetone before analysis. Freshly prepared ferric reducing antioxidant capacity reagent, containing 100 mM 2,4,6-tris(2-pyridyl)-*s*-triazine and 200 mM iron(III) chloride [$FeCl_3$] in sodium acetic buffer (pH 3.6–4), was added to both fractions. Measurement of the antioxidative capacity of the sample was based on its ability to reduce the yellow-colored Fe^{3+}–2,4,6-tris(2-pyridyl)-*s*-triazine complex to the blue-colored ferrous form, which was spectrophotometrically recorded at 593 nm. The results were calculated by standard curves prepared with

known concentrations of Trolox and expressed as micromoles of Trolox equivalents per gram fresh weight.

Antioxidant enzyme activities

Proteins were extracted from leaf samples by a 2-step ammonium sulfate precipitation method. All steps were performed at 4 °C. Leaf material was incubated for 30 min in fresh 0.1 M tris(hydroxymethyl)aminomethane–hydrogen chloride (Tris-HCl) buffer (pH 7.8), containing 5 mM EDTA, 5 mM dithioerythritol, 1% polyvinylpyrrilidone, and 1% Nonidet. After 30 min of centrifugation (50 000 *g*), the supernatant was incubated for 30 min with 40% ammonium sulfate ($[NH_4]_2SO_4$). After a second round of centrifugation, the supernatant was incubated for 30 min with 80% $(NH_4)_2SO_4$. The extract was subsequently desalted by running over PD-10 columns (2 min, 950 *g*, 4 °C) and directly stored at –80 °C for further analysis of enzyme activities. All enzyme activities were determined at 25 °C in 1-mL cuvettes. Eight biological replicates were used from each condition.

Superoxide dismutase (SOD) activity was determined in 33 mM monopotassium phosphate (KH_2PO_4) reaction buffer (pH 7.8) and 0.1 mM EDTA [30]. By adding 60 mU xanthine oxidase to 0.05 mM xanthine, uric acid is formed. In this reaction, superoxide is formed as a by-product and reduces cytochrome *c* (0.01 mM) in a blank sample. By adding plant extract, SOD activity is calculated indirectly by measuring the inhibition of formation of reduced cytochrome *c* at 550 nm. The amount of SOD inhibiting the production of reduced cytochrome *c* by 50% is defined as 1 unit of SOD activity.

Catalase (CAT) activity was determined in 75 mM KH_2PO_4 reaction buffer (pH 7) [31]. After addition of 1 mM H_2O_2, CAT activity is calculated by the rate at which H_2O_2 is reduced to H_2O and oxygen (O_2) and, hence, by measuring the decrease of H_2O_2 spectrophotometrically at 240 nm.

Glutathione reductase (GR) was determined in 1 mM Tris and 1 mM EDTA reaction buffer (pH 8) [31]. By adding 1.5 mM glutathione disulfide (GSSG) and 0.1 mM reduced nicotinamide adenine dinucleotide phosphate (NADPH) to the reaction buffer, GR present in the leaf extract catalyzes the reduction of GSSG to GSH, through simultaneous consumption of NADPH. Measuring the oxidation of NADPH at 340 nm makes it possible to calculate the GR activity.

Guaiacol peroxidase (GP*x*) was determined in 75 mM KH_2PO_4 reaction buffer (pH 7) [31]. Adding 1 mM H_2O_2 and 2 mM guaiacol to the reaction buffer, leaf extract catalyzes the conversion of H_2O_2 into H_2O and O_2 by oxidation of guaiacol, which was measured spectrophotometrically at 436 nm.

Syringaldazine peroxidase (SP*x*) was determined in 80 mM Tris-HCl reaction buffer (pH 7.5) [32]. Syringaldazine substrate (55 μM) was oxidized by SP*x* simultaneously with the reduction of 1 mM H_2O_2 and monitored at 530 nm.

Glutathione *S*-transferase activity was determined using different standard substrates: 1 mM 1-chloro-2,4-dinitrobenzene, 1 mM 1,2-dichloro-4-nitrobenzene, 1 mM 4-nitrobenzyl chloride, 1 mM *p*-nitrobenzoyl chloride, 0.5 mM *p*-nitrophenylacetate, and fluorodifen (1.2 mM) [33,34]. By adding 1 mM glutathione (GSH) to 1 mM of substrate in 75 mM KH_2PO_4 reaction buffer (pH 6.5), the formation of conjugate was measured at respective wavelengths (340 nm, 345 nm, 310 nm, 310 nm, 400 nm, and 400 nm).

Ascorbate peroxidase (AP*x*) activity was determined after a separate extraction [35]. Plant tissue (100 mg) was extracted using a modified extraction buffer, containing 0.1 M Tris-HCl (pH 7.8), 1 mM dithiothreitol (DTT), 1 mM EDTA, and 10 mM ascorbate. Ascorbate peroxidase reduces H_2O_2 by oxidation of ascorbate into dehydroascorbate. Adding 20 mM H_2O_2 to the reaction buffer (0.1 M *N*-[2-hydroxyethyl]piperazine-*N*′-ethanesulfonic acid and 1 M EDTA, pH 7) made it possible to calculate AP*x* activity in leaf extract by monitoring the decrease of ascorbate at 298 nm.

Metabolite concentration and redox state

Leaf tissue was extracted in 200 mM HCl. After centrifugation (16 000 *g*, 10 min, 4 °C), the supernatant was diluted with 200 mM NaH_2PO_4 (pH 5.6) and brought to pH 4.5 by addition of 200 mM Na hydroxide. This extract was used for determination of both ascorbate and GSH concentrations and their redox state [36]. Eight biological replicates were used from each condition. Ascorbate determination was based on ascorbate oxidase–mediated oxidation of ascorbate. Dithiothreitol (25 mM) was added to one-half of the leaf extract, reducing all present dehydroascorbate. By addition of ascorbate oxidase to the subsample without DTT and the subsample with DTT, the reduced fraction (ascorbate) and the total fraction of ascorbate (ascorbate and dehydroascorbate) could be determined by spectrophotometric measurement of the decrease in reduced ascorbate at 265 nm. Glutathione measurement was based on GSH-mediated reduction of 5,5′-dithiobis-2-nitrobenzoic acid, which was analyzed using a spectrophotometer at 412 nm. By incubating half of the plant extract with 2-vinylpiridine for 30 min at 20 °C, GSH was inactivated and only the present oxidized fraction of glutathione (GSSG) could be measured. By addition of GR to both incubated and nonincubated subsamples, GSSG and total GSH concentrations could be determined by monitoring the reduction of 5,5′-dithiobis-2-nitrobenzoic acid by GSH.

Metazachlor determination in leaves

Metazachlor was determined in aboveground biomass via reverse-phase high-performance liquid chromatography (HPLC; Adept CE-4200, Dual Piston Pump CE 4120, UV/VIS detector and Power Stream software). For extraction, 5 g of fresh plant tissue was homogenized in 5 mL pure acetonitrile (HPLC-grade; J.T. Baker). To improve the recovery of polar components and to facilitate the partitioning of the solvent, 2 g magnesium sulfate ($MgSO_4$) was added to the extract. To reduce the amount of polar interferences, 0.5 g NaCl was added. By addition of 0.5 g Na_3 citrate $\times$ 2 H_2O and 0.25 g Na_2H citrate $\times$ 1.5 H_2O, the optimal pH of 6.5 was maintained. The extract was centrifuged for 5 min at 1057 *g* at room temperature. One milliliter of supernatant was transferred to a dispersive centrifuge tube (Spectrum® Chemical MFG) containing 25 mg of primary secondary amine, 150 mg $MgSO_4$, and 2.5 mg of graphitized carbon black to remove pigments. The tubes were mixed for 30 s and then centrifuged again for 5 min at 1057 *g*. Subsequently, the collected supernatant was analyzed by reverse-phase HPLC. Samples were analyzed at 220 nm in a gradient regime by an analytical column Supelcosil LC-18 150 $\times$ 4.6 mm, 5 μm. The injected volume was 20 μL. The mobile phase composition was phase A acetonitrile:water (40:60) and phase B acetonitrile:water (80:20). The gradient was applied for 20 min in the following regime: 0 min, 100% A:0% B; 10 min, 50% A:50% B; 20 min, 0% A:100% B, with a flow rate of 1 mL/min. The limit of quantification and the limit of detection of this analytical method were 1.1 μg/mL and 0.4 μg/mL, respectively. Quantification was based on a metazachlor standard curve prepared with certified metazachlor standard (98.5%; Dr. Ehrenstorfer).

Nutrient profile in leaves

Dry leaf material (0.1–0.5 g) was digested in 70% to 71% nitric acid and dissolved in 2% HCl. After digestion, the clear colorless extract was brought to 25-mL volume with Milli-Q water. Macronutrients (phosphorus [P], K, magnesium [Mg], calcium [Ca], sulfur [S]) and micronutrients (Na, Fe, copper [Cu], zinc [Zn], manganese [Mn]) present in plant extracts were determined by ICP-OES (710; Agilent Technologies). Concentrations were calculated by the use of standard curves with known concentrations.

Statistical analyses

All data were subjected to one-way or two-way analysis of variance (ANOVA) in open-source R software (R Ver 3.1.2, R Foundation for Statistical Computing), in strict accordance to parametrical conditions. Normal distribution of the data was tested using the Shapiro-Wilk test. Following the ANOVA, a post hoc Tukey test was performed for multiple pairwise comparisons. Where parametric conditions were not met, Kruskal-Wallis followed by 2-by-2 Wilcoxon post hoc comparison analyses were performed. Data are represented as mean values ± standard error, and significance was set at the 5% level.

RESULTS

Growth, development, and morphology of B. napus

Seven days after metazachlor application, seed germination was 10% lower in microcosms treated with 0.2 mM and 0.4 mM metazachlor in comparison to nontreated microcosms, although not significantly different at the $p < 0.05$ level (data not shown). Two weeks after treatment (14 d after treatment) 1.12 mg and 1.58 mg metazachlor/kg fresh weight were found in the aerial parts of 0.2 mM and 0.4 mM metazachlor-treated plants, respectively. During the following 4 wk, the levels of metazachlor decreased by 78% and 64% in the aerial plant parts of the respective treatments to 0.24 mg and 0.57 mg metazachlor/kg fresh weight (42 d after treatment; Figure 1). Soon after application, leaves displayed fasciation in the form of crinkled leaves, shortened mid-ribs, and incomplete detachment of leaves under the influence of metazachlor (Figure 2). These malformations appeared within the first 2 wk to 6 wk after treatment and remained present until leaf abscission during further development. Twenty-one days after treatment, 20% and 50% of the plants treated with 0.2 mM and 0.4 mM metazachlor, respectively, displayed signs of fasciation and 20% of the plants

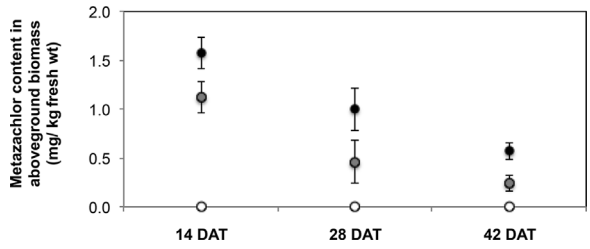

Figure 1. Metazachlor concentration in aboveground plant parts of *Brassica napus* 14 d, 28 d, and 42 d after treatment with 0 mM, 0.2 mM, and 0.4 mM metazachlor. Data are presented as average values of a minimum of 3 biological replicates ± standard error. DAT = days after treatment.

in both treatments did not survive the first 7 wk (data not shown). Weight and height were strongly inhibited in 0.2 mM and 0.4 mM metazachlor-exposed plants at 14 d after treatment in a dose-dependent way (Figures 3A and 4 and Table 1). These differences were still evident at 28 d after treatment (Figure 3B and Table 2); but at 63 d after treatment, fresh weights of plants under different exposures were equal (Figure 3C). The rate of development of leaves of the young seedlings showed no apparent differences up to 5 wk after metazachlor application (35 d after treatment; Figure 5). However, considering leaf surface area and petiole length, the leaves appeared to be smaller under the influence of metazachlor, with smaller leaf surface area and shorter petioles, which might explain the reduction in aboveground weight in the short term (Supplemental Data, Figure S1). Between 5 wk and 7 wk after application, metazachlor-exposed plants tended to develop leaves faster than control plants. At 47 d after treatment, for example, 30% and 70% of 0.2 mM and 0.4 mM metazachlor-exposed plants, respectively, had reached growth stage 19 or 20 and, thus, had developed 9 or more leaves, whereas all control plants had developed a maximum of 8 leaves (Figure 5).

Enzymes and metabolites involved in detoxification

The activity of GST significantly increased under the influence of metazachlor at 14 d and 28 d after treatment (Tables 1 and 2 and Figure 6). The activity of GST was increased toward 1-chloro-2,4-dinitrobenzene, fluorodifen, and nitrophenylacetate substrates and not found for 1,2-dichloro-4-nitrobenzene, 4-nitrobenzyl chloride, and *p*-nitrobenzoyl chloride, with the strongest induction toward 1-chloro-2,4-dinitrobenzene (Tables 1 and 2). At both time points, the level of GSH, which is consumed during GST–catalyzed metabolization of xenobiotics such as herbicides, tended to be lower under the

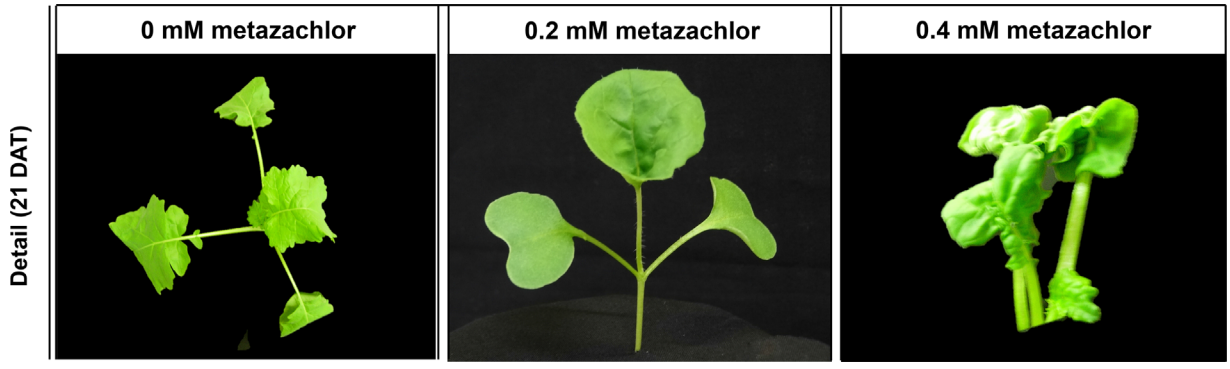

Figure 2. Detailed images of *Brassica napus* exposed to 0 mM, 0.2 mM, and 0.4 mM metazachlor at 21 d after treatment. Plants exposed to 0.2 mM and 0.4 mM metazachlor displayed malformations of the leaves. DAT = days after treatment.

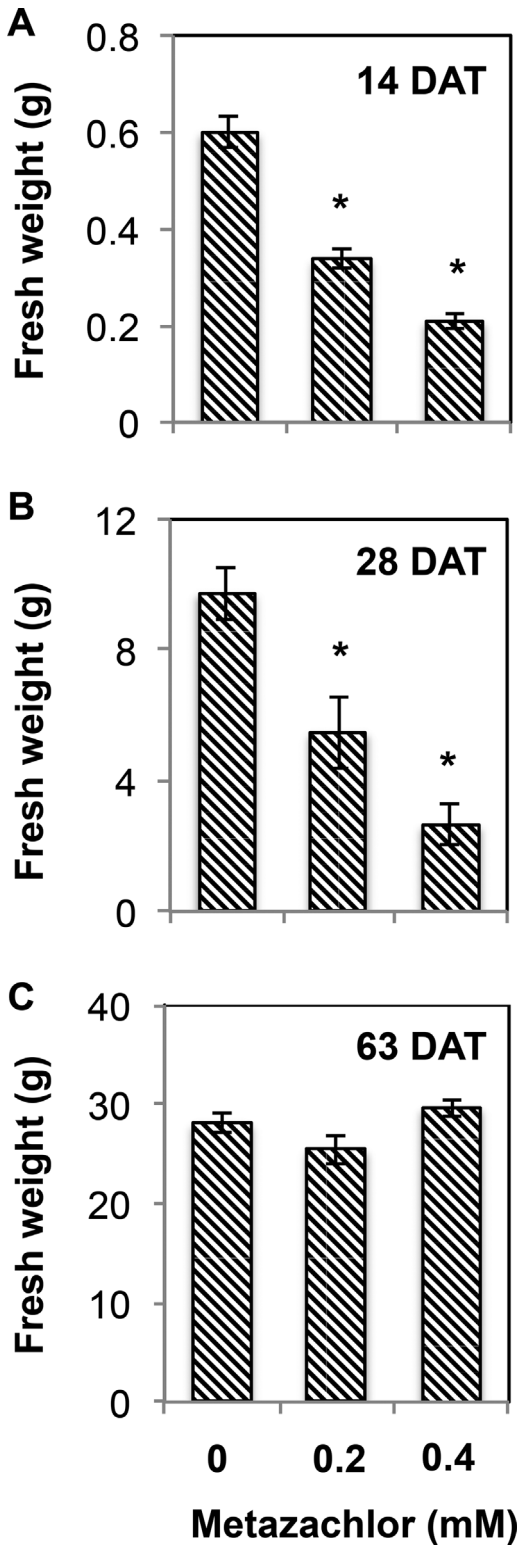

Figure 3. Aboveground fresh weight of *Brassica napus* 14 d after treatment (**A**), 28 d after treatment (**B**), and 63 d after treatment (**C**) with 0 mM, 0.2 mM, and 0.4 mM metazachlor. Data are presented as average values of a minimum of 10 biological replicates ± standard error (*post hoc values $p < 0.05$). DAT = days after treatment.

influence of metazachlor (Figure 6). Whereas this trend could not be statistically underpinned, the redox state of glutathione was significantly turned toward the oxidized form (GSSG) at 14 d after treatment under the influence of 0.4 mM metazachlor (Table 1). At 28 d after treatment, the redox state of GSH was similar in all treatments.

Metazachlor induces oxidative stress in the leaves of B. napus

The presence of reactive oxygen species (ROS; e.g., H_2O_2) was visualized using 3,3′-diaminobenzidine staining. No differences in the presence of H_2O_2 were detected at 14 d after treatment because 3,3′-diaminobenzidine staining was restricted to the veins in all conditions (Supplemental Data, Figure S2). At 14 d after treatment, the total antioxidative capacity in the leaves of *B. napus* tended to increase under the influence of metazachlor; however, this trend could not be statistically supported (Table 1). At 28 d after treatment, a significant increase in the lipophilic fraction of antioxidants was observed (Table 2). In addition, the activities of enzymes involved in the antioxidative defense (SOD, CAT, AP*x*, and GR) and cell wall lignification (GP*x* and SP*x*) were measured. In general, the activities of all antioxidative enzymes increased with exposure to increasing metazachlor doses (Tables 1 and 2). A higher activity in metazachlor-treated plants in comparison to nontreated plants could be statistically confirmed for CAT, AP*x*, and SP*x*, at 14 d after treatment and for SOD, CAT, GR, and GP*x* at 28 d after treatment. Twenty-eight days after treatment, the levels of ascorbate were not affected by the applied metazachlor treatments. Together with ascorbate, GSH is a key metabolite in the ascorbate–GSH cycle, a supportive cycle behind the enzymatic antioxidative defense. The redox state of GSH was significantly leaning toward the oxidized form (GSSG) under the influence of 0.4 mM metazachlor at 14 d after treatment.

Metazachlor induces membrane lipid peroxidation and shifts in pigment and nutrient profiles

The increasing trend in thiobarbituric acid–reactive metabolites of 39% and 43% in 0.2 mM and 0.4 mM metazachlor-exposed plants, respectively, indicated that cellular membranes were destabilized by lipid peroxidation at 28 d after treatment (Table 2). No clear shifts in pigment profile were observed 2 wk after application. Twenty-eight days after treatment, however, the pigment profile in *B. napus* leaves was influenced by 0.2 mM metazachlor with an increased chlorophyll concentration because of an increment of chlorophyll *a* (Table 2). Fourteen-day-old plants exposed to 0.4 mM metazachlor contained higher nutrient levels in their aboveground areal parts. Levels of macronutrients, such as K, Ca, and P, as well as of micronutrients, such as Mn and Cu, increased significantly within a range of 25% to 80% under the influence of 0.4 mM metazachlor (Table 1). Twenty-eight days after treatment, the nutrient profile in metazachlor-treated plants differed from that of control plants, with significant losses of P and significant augmentation of Mg and Na (Table 2).

DISCUSSION

In the present study, controlled growth experiments of oilseed rape were carried out using microcosms in temperature-controlled, light-controlled, and moisture-controlled growth chambers. This experimental setup enabled us to investigate the specific impact of metazachlor on the crop *B. napus*, with exclusion of the complex interaction with soil characteristics and soil organisms, the direction and rate of drainage, and the presence of herbivores, such as snails. Hence, the underlying

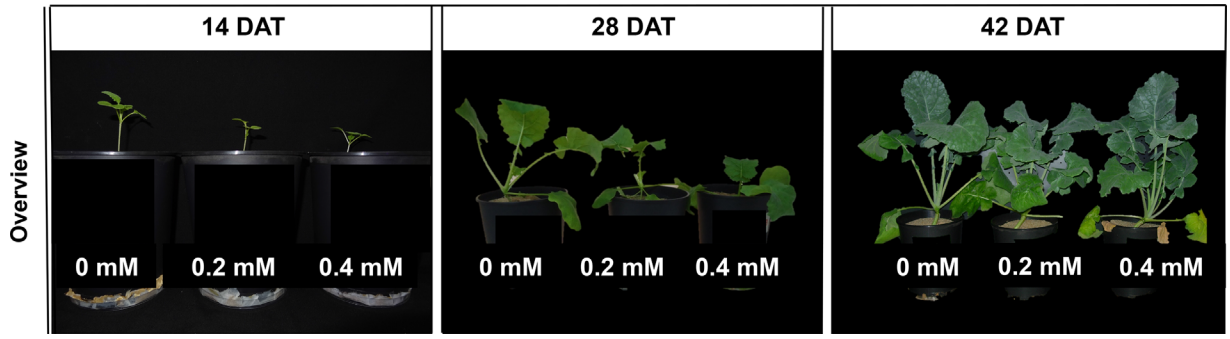

Figure 4. Overview images of *Brassica napus* exposed to 0 mM, 0.2 mM, and 0.4 mM metazachlor at 14 d, 28 d, and 42 d after treatment. DAT = days after treatment.

mechanisms that ultimately determine the degree of phytotoxicity could be studied.

Detoxification metabolism in B. napus *is activated 2 wk to 4 wk after metazachlor application*

The detoxification capacity of a crop is crucial for the neutralization of xenobiotic compounds and ultimately determines the potential harm induced by that compound, either in the form of direct interaction or via the induction of oxidative stress. The presence of metazachlor in the aboveground organs of young oilseed rape seedlings pointed out that metazachlor was taken up by roots and translocated into the shoots within 2 wk after application. The decrease of the internal metazachlor concentration in the aboveground parts of *B. napus* during the subsequent weeks indicated activation of the detoxification metabolism (Figure 1). The rate of detoxification decreased with increasing metazachlor dose 2 wk after application, which might indicate either that the detoxification metabolism is suppressed by the high internal metazachlor concentration or that it reached its maximal turnover (Figure 1). Taking into account the rate of detoxification, extrapolation of the results of this laboratory test setup suggests that metazachlor might be entirely metabolized internally within 10 wk to 12 wk after application (Figure 1). This result is in line with reported half-lives of metazachlor in the soil of 19 d to 82 d [37]. In general, the detoxification rate of herbicides is determined by the activity of cytochrome P450 peroxidases, GSH, and GST. The detoxification of chloroacetamides does not involve phase I metabolization by cytochrome P450 and is only facilitated by GST–mediated conjugation [38]. However, the tolerance of a crop toward a certain herbicide is not solely determined by the activity of GST. Glutathione concentration and redox state are also important [10]. After metazachlor application, the increased activity of GST at both time points and the increment in GSSG fraction at 14 d after treatment suggest that the detoxification of metazachlor was activated in oilseed rape (Figure 6). Two weeks after metazachlor application, the increased activity of GST with affinity toward 1-chloro-2,4-dinitrobenzene and nitrophenylacetate substrates indicates that metazachlor and its metabolites were being conjugated with GSH prior to storage in the cell wall or in the vacuole (Figure 6). Four weeks after application, GST showed affinity to all tested GST substrates (Figure 6). Phi class GST's are closely associated with detoxification of chloroacetamides [17]. Because fluorodifen has been associated with tau class GST activity [39] and 1-chloro-2,4-dinitrobenzene is considered a nonspecific substrate [11], it can be considered that both tau and phi classes of GSTs, which are the most important routes for detoxification in plants [40], are involved in detoxification of metazachlor. Because the glutathione redox state is promoted toward its oxidized form (GSSG) under metazachlor treatment, GSH biosynthesis might not be able to provide the demand for GSH at this time point (Table 1). Two weeks later, the augmented activity of GST indicates that glutathione is still actively consumed for metazachlor conjugation at this time point (Table 2 and Figure 6). In accordance with the present results, the related chloroacetamide metolachlor induced a 5-fold increase in GST activity in maize [41]. Although Viger et al. [41] did not observe any changes in GSH content, Štajner et al. [20] noticed decreased GSH contents in lettuce, pea, and bean seeds under the influence of chloroacetamides, alachlor and metolachlor.

Metazachlor-induced oxidative stress results in membrane damage of plant cells

The presence of ROS, such as H_2O_2, in leaves of metazachlor-exposed seedlings could not be revealed with the 3,3′-diaminobenzidine staining technique. However, the increased activity of enzymes involved in antioxidative defense and cell wall lignification and the activation of the ascorbate–GSH cycle indirectly suggest the induction of pro-oxidants under the influence of metazachlor 2 wk and 4 wk after application (Tables 1 and 2 and Figure 6). The total antioxidative capacity in leaf cells, determined by the ferric reducing antioxidative capacity, comprises both water-soluble antioxidants, such as GSH, ascorbate, proline, phenolic compounds, and membrane-bound molecules, as well as water-insoluble antioxidants, such as carotenoids and tocopherols (vitamin E) [42]. The increase of the lipophilic fraction of antioxidants and the increase of carotenoid concentration at 28 d after treatment (Table 2) suggest a potential role for tocopherols as antioxidative compounds at this time point. Tocopherols have a significant role in herbicide-induced oxidative stress because of their ability to protect membrane-localized polyunsaturated fatty acids against ROS–induced lipid peroxidation [43,44]. However, the simultaneous increase in lipid peroxidation suggests insufficient protection of leaf tissue against oxidative stress. Membrane integrity was estimated via K leakage and lipid peroxidation. The latter was significantly induced by metazachlor at 28 d after treatment (Table 2). Whereas the destabilization of membranes can directly be induced through the inhibition of fatty acid biosynthesis by metazachlor, this also can be the result of metazachlor-induced oxidative stress. That these responses in membrane destabilization became significant after 4 wk could be explained by either the fact that the inhibition of very long chain fatty acids is a relatively slow process [23] or the fact that oxidative damage is a secondary side

Table 1. Growth, membrane damage, pigment and nutrient profile, antioxidative defense, and detoxification in *Brassica napus* leaves 14 d after treatment with 0 mM, 0.2 mM, and 0.4 mM metazachlor

		Metazachlor treatment[a]		
Response level	Unit	0 mM	0.2 mM	0.4 mM
Growth				
Shoot weight	mg	599 ± 31	338 ± 19*	209 ± 15*
Root weight	mg	119 ± 9	52 ± 4*	28 ± 2*
Shoot length	cm	4.4 ± 0.3	2.4 ± 0.1*	1.7 ± 0.2*
Root length	cm	12.0 ± 0.5	6.0 ± 0.5*	3.1 ± 0.3*
Antioxidant defense and detoxification				
Total antioxidative capacity	μmol Trolox eq./g fresh wt	18 ± 2	23 ± 1	23 ± 2
Hydrophilic fraction AO	μmol Trolox eq./g fresh wt	15 ± 2	20 ± 1	20 ± 1
Lipophilic fraction AO	μmol Trolox eq./g fresh wt	2.8 ± 0.3	3.3 ± 0.3	3.9 ± 0.8
Antioxidative enzymes				
Superoxide dismutase	mU/g fresh wt	293 ± 32	379 ± 45	370 ± 73
Catalase	mU/g fresh wt	7.5 ± 1.4	13.5 ± 1.8*	9.4 ± 1.4
Ascorbate peroxidase	U/g fresh wt	38 ± 3.4	54 ± 0.9	52 ± 9.8
Glutathione reductase	mU/g fresh wt	470 ± 48	671 ± 97	863 ± 140
Syringaldazine peroxidase	mU/g fresh wt	39 ± 6	178 ± 74*	241 ± 38*
Guaiacol peroxidase	mU/g fresh wt	47 ± 3.4	127 ± 37	109 ± 36
Antioxidative metabolites				
Total ascorbate	μmol/g fresh wt	4.3 ± 0.7	4.3 ± 0.5	5.7 ± 0.6
Oxidized ascorbate	DHA/AsA ratio	0.19 ± 0.04	0.13 ± 0.02	0.13 ± 0.04
Glutathione	nmol/g fresh wt	515 ± 57	428 ± 32	465 ± 66
Oxidized glutathione	GSSG/GSH ratio	0.034 ± 0.006	0.049 ± 0.012	0.069 ± 0.008*
Detoxifying enzymes				
GST-CDNB	mU/g fresh wt	102 ± 3	178 ± 41	235 ± 32*
GST-Fluorodifen	mU/g fresh wt	4.1 ± 0.5	5.9 ± 1.1	6.2 ± 1.1
GST-Npa	mU/g fresh wt	21 ± 2	34 ± 1*	35 ± 6
Membrane damage				
TBA reactive molecules	nmol/g fresh wt	30 ± 3	33 ± 2	37 ± 4
Potassium leakage	% extracellular K	5.8 ± 0.3	7.7 ± 1.4	5.1 ± 1.4
Pigment and nutrient profile				
Pigment profile				
Chlorophyll *a*	mg/g fresh wt	1.1 ± 0.2	1.4 ± 0.1	1.5 ± 0.1
Chlorophyll *b*	mg/g fresh wt	0.63 ± 0.08	0.82 ± 0.06	0.81 ± 0.06
Chlorophyll *a/b*		1.9 ± 0.02	1.7 ± 0.1	1.8 ± 0.2
Total chlorophyll	mg/g fresh wt	1.8 ± 0.2	2.2 ± 0.1	2.3 ± 0.2
Carotenoids	mg/g fresh wt	0.16 ± 0.01	0.16 ± 0.02	0.23 ± 0.04
Chlorophyll/carotenoids		11 ± 1	15 ± 3	11 ± 2
Nutrient content				
Macronutrnts				
Potassium	mg/g dry wt	30 ± 1	31 ± 0.4	39 ± 1*
Calcium	mg/g dry wt	20 ± 1	21.2 ± 0.3	26 ± 1*
Phosphorus	mg/g dry wt	12 ± 0.3	13 ± 0.5	15 ± 0.3*
Sulfur	mg/g dry wt	11 ± 0.3	12 ± 0.2	12 ± 1
Magnesium	mg/g dry wt	3.7 ± 0.2	3.9 ± 0.1	4.4 ± 0.2
Micronutrients				
Sodium	mg/g dry wt	1.2 ± 0.1	1.3 ± 0.1	1.0 ± 0.04
Iron	μg/g dry wt	438 ± 104	489 ± 275	171 ± 19
Manganese	μg/g dry wt	76 ± 3	82 ± 1	137 ± 7*
Zinc	μg/g dry wt	29 ± 5	29 ± 3	41 ± 2
Copper	μg/g dry wt	4.2 ± 0.4	4.4 ± 0.1	7.2 ± 0.3*

[a]Data are shown as average values of a minimum of 4 biological replicates ± standard error.
*Post hoc values $p < 0.05$.
AO = ascorbate oxidase; AsA = ascorbate; CDNB = 1-chloro-2,4-dinitrobenzene; DHA = dehydroascorbate; GSH = reduced glutathione; GSSG = oxidized glutathione; GST = glutathione *S*-transferase; Npa = nitrophenylacetate; TBA = thiobarbituric acid.

effect of metazachlor. In general, herbicide-induced oxidative stress has been described in several crops [18,19], in particular for chloroacetamides such as alachlor and metolachlor [20,21]. The induction of the antioxidative enzymes SOD, AP_X, CAT, and GR at 2 wk and 4 wk after metazachlor application indicated metazachlor-induced oxidative stress (Tables 1 and 2). The reduced CAT activity in the highest metazachlor treatment at 14 d after treatment could be linked to the high phytotoxic effects of metazachlor. However, the high sensitivity of CAT toward high levels of H_2O_2 has been described in different crop species under the influence of various stresses, such as Cu [45], herbicides [46] and high and low temperatures [47]. The high activities of cell wall–bound peroxidases that use syringaldazine and guaiacol as substrates (Tables 1 and 2) and that are involved in lignin biosynthesis suggest either the apoplastic presence of ROS or the activation of cell wall lignification [48,49]. Increased cell wall lignification could result in a reduced permeability by the establishment of a physical barrier and can therefore allow the cell to better protect itself against xenobiotics. Lignin is known to be responsive to a range of

Table 2. Growth, membrane damage, pigment and nutrient profile, antioxidative defense, and detoxification in *Brassica napus* leaves 28 d after treatment with 0 mM, 0.2 mM, and 0.4 mM metazachlor

		Metazachlor treatment[a]		
Response level	Unit	0 mM	0.2 mM	0.4 mM
Growth				
Shoot weight	g	9.7 ± 0.8	5.5 ± 1.1*	2.6 ± 0.6*
Root weight	g	2.8 ± 0.6	0.9 ± 0.3*	0.2 ± 0.1*
Shoot length	cm	4.7 ± 0.6	2.5 ± 0.2*	1.6 ± 0.1*
Root length	cm	29 ± 2	19 ± 1*	12 ± 1*
Antioxidant defense and detoxification				
Total antioxidative capacity	μmol Trolox eq./g fresh wt	24 ± 1	27 ± 2	28 ± 1
Hydrophilic fraction AO	μmol Trolox eq./g fresh wt	18 ± 1	18 ± 2	18 ± 1
Lipophilic fraction AO	μmol Trolox eq./g fresh wt	5.7 ± 0.7	9.1 ± 0.9*	10 ± 0.4*
Antioxidative enzymes				
Superoxide dismutase	mU/g fresh wt	261 ± 18	305 ± 13	441 ± 32*
Catalase	mU/g fresh wt	13 ± 3	27 ± 1	37 ± 6*
Ascorbate peroxidase	U/g fresh wt	8.4 ± 2	12 ± 1	14 ± 3
Glutathione reductase	mU/g fresh wt	394 ± 6	516 ± 40*	644 ± 63*
Syringaldazine peroxidase	mU/g fresh wt	108 ± 35	177 ± 24	169 ± 15
Guaiacol peroxidase	mU/g fresh wt	35 ± 15	43 ± 6	112 ± 25*
Antioxidative metabolites				
Total ascorbate	μmol/g fresh wt	0.88 ± 0.20	0.95 ± 0.17	0.95 ± 0.15
Oxidized ascorbate	DHA/AsA ratio	0.15 ± 0.07	0.61 ± 0.18	0.50 ± 0.18
Glutathione	nmol/g fresh wt	276 ± 148	151 ± 15	148 ± 14
Oxidized glutathione	GSSG/GSH ratio	0.028 ± 0.014	0.027 ± 0.010	0.035 ± 0.013
Detoxifying enzymes				
GST-CDNB	mU/g fresh wt	69 ± 19	116 ± 11	148 ± 19*
GST-Fluorodifen	mU/g fresh wt	3.0 ± 0.6	5.0 ± 0.8	7.2 ± 1.4*
GST-Npa	mU/g fresh wt	22 ± 1.0	28 ± 2	34 ± 2*
Membrane damage				
TBA reactive molecules	nmol/g fresh wt	23 ± 2	32 ± 2*	33 ± 3*
Potassium leakage	% extracellular K	8.4 ± 1.6	5.6 ± 1.4	14 ± 2
Pigment and nutrient profile				
Pigment profile				
Chlorophyll *a*	mg/g fresh wt	0.81 ± 0.02	0.95 ± 0.05*	0.89 ± 0.03
Chlorophyll *b*	mg/g fresh wt	0.24 ± 0.003	0.27 ± 0.01	0.27 ± 0.01
Chlorophyll *a*/*b*		3.5 ± 0.1	3.6 ± 0.1	3.3 ± 0.1
Total chlorophyll	mg/g fresh wt	1.05 ± 0.06	1.22 ± 0.06*	1.15 ± 0.03
Carotenoids	mg/g fresh wt	0.145 ± 0.004	0.164 ± 0.008	0.162 ± 0.004*
Chlorophyll/carotenoids		7.2 ± 0.1	7.4 ± 0.2	7.1 ± 0.4
Nutrient content				
Macronutrients				
Potassium	mg/g dry wt	56 ± 5	47 ± 2	45 ± 1
Calcium	mg/g dry wt	26 ± 2	30 ± 2	30 ± 2
Phosphorus	mg/g dry wt	7.3 ± 0.2	4.6 ± 1.5*	6.1 ± 0.3*
Sulfur	mg/g dry wt	14 ± 1	15 ± 1	14 ± 1
Magnesium	mg/g dry wt	5.5 ± 0.2	7.0 ± 0.2*	7.1 ± 0.3*
Micronutrients				
Sodium	mg/g dry wt	1.4 ± 0.1	2.7 ± 0.1*	2.3 ± 0.2*
Iron	μg/g dry wt	204 ± 25	295 ± 62	230 ± 58
Manganese	μg/g dry wt	101 ± 18	155 ± 10	114 ± 30
Zinc	μg/g dry wt	39 ± 5	60 ± 3*	16 ± 5*
Copper	μg/g dry wt	4.3 ± 0.5	4.3 ± 0.1	3.5 ± 0.2

[a]Data are shown as average values of a minimum of 4 biological replicates ± standard error.
*Post hoc values $p < 0.05$.
AO = ascorbate oxidase; AsA = ascorbate; CDNB = 1-chloro-2,4-dinitrobenzene; DHA = dehydroascorbate; GSH = reduced glutathione; GSSG = oxidized glutathione; GST = glutathione *S*-transferase; Npa = nitrophenylacetate; TBA = thiobarbituric acid.

stresses. Biotic and abiotic stresses (such as metals) are known to induce lignification in the walls of cells that do not lignify under nonstress responses [50]; however, this has not been described yet for herbicides. The increased activity of AP*x* under the influence of 0.2 mM metazachlor at 14 d after treatment indicates that H_2O_2 is being converted actively into water and oxygen (Figure 6) and suggests activation of the ascorbate–GSH cycle. This assumption is supported by the significant shift of the glutathione redox state toward its oxidized form, GSSG, at 14 d after treatment and the increased activity of GR at 28 d after treatment under the influence of metazachlor (Figure 6). Together with glutathione's shift toward its oxidized form, the increased activity of GST implies that GSH is consumed in the detoxification metabolism of metazachlor. Therefore, it can be presumed that GSH fulfills a dual role in both antioxidative defense and detoxification (Figure 6). Although ROS are known to induce oxidative damage, they also have an important function in signaling [51].

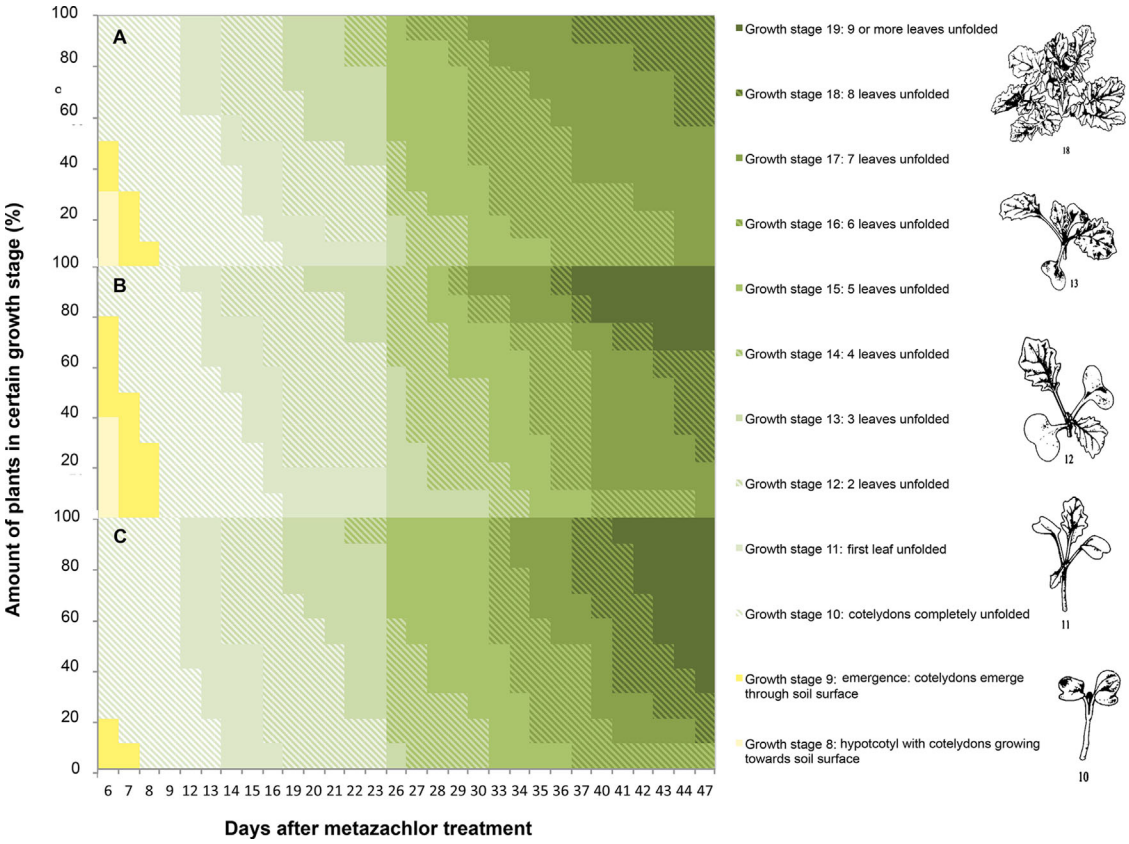

Figure 5. Emergence and leaf development of *Brassica napus* over time, treated with (**A**) 0 mM, (**B**) 0.2 mM, and (**C**) 0.4 mM metazachlor, expressed as the percentage of all measured plants at a specific developmental stage at a defined time point (days after treatment). Different growth stages are depicted as described by Lancashire et al. [25].

Hydrogen peroxide has been shown to regulate GST in vivo [52] and can therefore influence the rate of detoxification. Glutathione *S*-transferase induction by ROS would appear to represent an adaptive response because these enzymes detoxify some of the toxic carbonyl-containing, peroxide-containing, and epoxide-containing metabolites produced within the cell by oxidative stress [53].

Metazachlor inhibits growth, induces fasciation, and causes membrane peroxidation in the short term

Phytotoxic effects of metazachlor on oilseed rape became apparent shortly after its application, with a reduction of germination (data not shown), the manifestation of fasciation (Figure 2), and the occurrence of mortality (data not shown). Fasciation of the leaves was already induced immediately after seedling emergence (Figure 2). Typical symptoms of chloroacetamide herbicides, such as stunted growth, cupped and wrinkled leaves, shortened main veins, and leaf fasciation, were induced, as formerly observed in *Arabidopsis thaliana* exposed to the related chloroacetamides acetolachlor, alachlor, and metolachlor [5]. Metazachlor-induced fasciation could be attributed to the mode of action of chloroacetamides, whereby inhibition of very long chain fatty acid synthesis has led to the inhibition of normal cell division [54,55]. During the further development of the crop, stem and shoot weights of the emerged seedlings were suppressed by metazachlor (Figure 3 and Tables 1 and 2). Reductions in crop shoot length have been observed in *Sorghum* sp. under the influence of the chloroacetamide metolachlor [56]. Although the timing of appearance of the leaves of *B. napus* seedlings seemed not to be influenced by metazachlor (Figure 5), the surface of the leaves and the petiole length were noticeably reduced (Supplemental Data, Figure S1) and could be linked with an insufficient capacity of light capitation for photosynthesis and therefore reduced shoot weight. However, the pigment profile was not influenced as such (Tables 1 and 2). In contrast to previous studies where pigment content was negatively affected by pesticides [8,57], chlorophyll and carotenoid concentrations rather tended to increase under the influence of metazachlor (Tables 1 and 2). Although metazachlor did not have any effect on the rate of leaf development up to 5 wk after treatment, metazachlor-exposed plants tended to develop leaves faster than control plants between 5 wk and 7 wk after treatment (Figure 5). Taking into consideration the development of leaves and the similar weights of metazachlor exposed and nonexposed seedlings 9 wk after application (Figure 3C), the seedlings appeared to recover from the initial herbicide stress by investing in leaf development.

CONCLUSIONS

In conclusion, this controlled microcosm experiment demonstrated that, in the short term, metazachlor induces significant adverse effects on oilseed rape at the morphological level. Together with an induction of the detoxification metabolism and the activation of the antioxidative defense responses, a reduction in growth investment was observed. These observations underpin the hypothesis that plants are investing energy in detoxification of the absorbed metazachlor and in neutralization of metazachlor-induced ROS over shoot

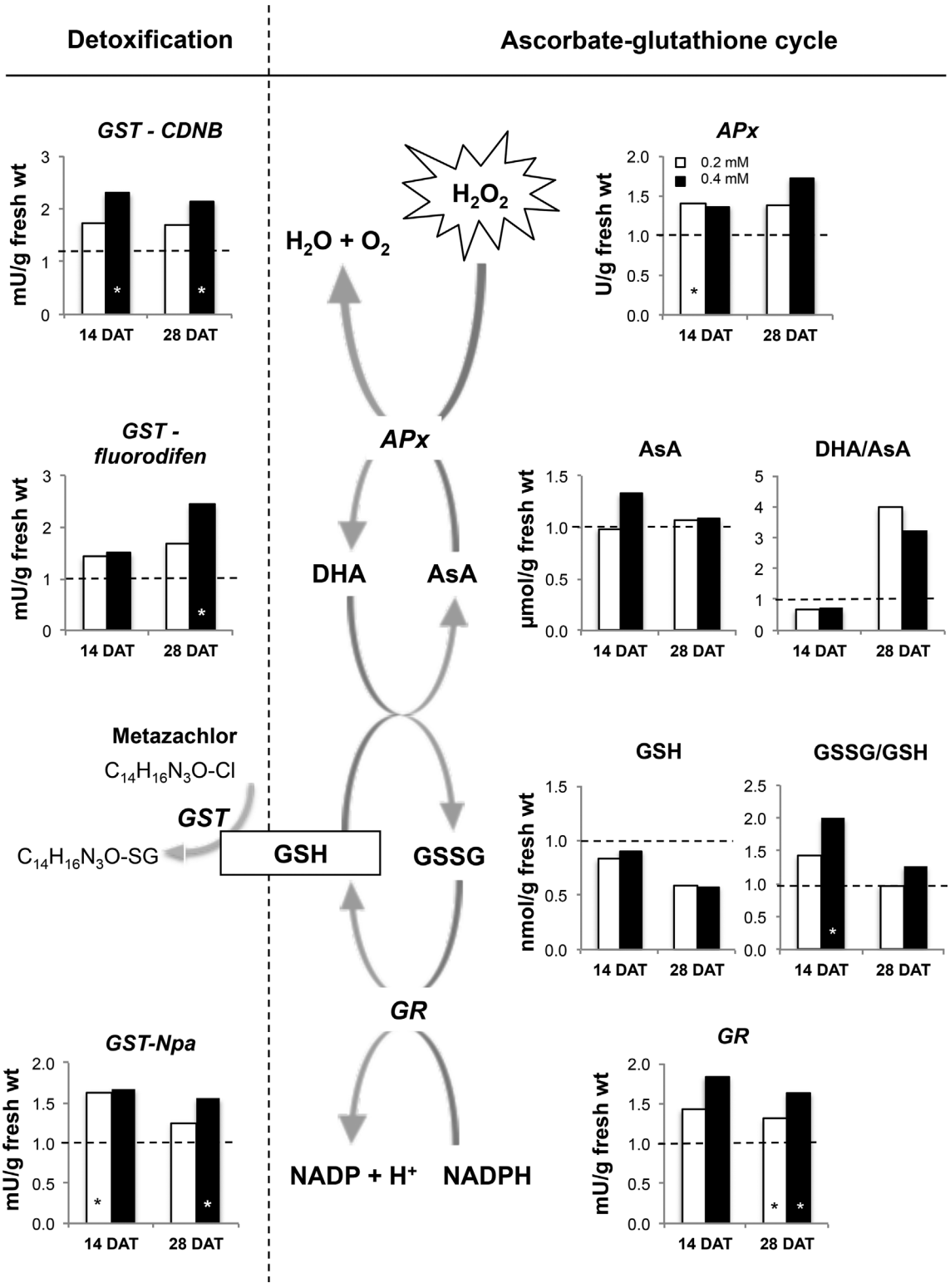

Figure 6. An overview of the relative enzyme activities and metabolite concentrations that play a role in either the detoxification of herbicides or the antioxidant defense mechanism (*post hoc value $p < 0.05$). Data are expressed relative to control values (dashed line). AP*x* = ascorbate peroxidase; AsA = ascorbate; CDNB = chlorodinitrobenzene; DAT = days after treatment; DHA = dehydroascorbate; GR = glutathione reductase; GSH = glutathione; GSSG = glutathione disulfide; GST = glutathione *S*-transferase; NADPH = nicotinamide adenine dinucleotide phosphate; Npa = nitrophenylacetate.

growth. This strategy seems to suffice for the plants to recover because 9 wk after application their weight no longer differed from that of nontreated plants. When considering the weight of the aboveground aerial plant parts, metazachlor-exposed plants appear to be able to recover from the initial chemical-induced stress.

Supplemental Data—The Supplemental Data are available on the Wiley Online Library at DOI: 10.1002/etc.3538.

Acknowledgment—We thank A. Wijgaerts and C. Put for their technical assistance in the microcosm experiment. The present study was supported by a PhD grant from the Institute for the Promotion of Innovation through Science and Technology in Flanders (IWT-Vlaanderen, to H. Vercampt).

We especially thank G. Chotoklieva for technical assistance in the metazachlor analyses.

REFERENCES

1. Fuerst EP. 1987. Understanding the mode of action of the chloroacetamide and thiocarbamate herbicides. *Weed Technol* 1:270–277.
2. Mamy L, Barriuso E, Gabrielle B. 2005. Environmental fate of herbicides trifluralin, metazachlor, metamitron and sulcotrione compared with that of glyphosate, a substitute broad spectrum herbicide for different glyphosate-resistant crops. *Pest Manag Sci* 61:905–916.
3. Carpenter D, Boutin C. 2010. Sublethal effects of the herbicide glufosinate ammonium on crops and wild plants: Short-term effects compared to vegetative recovery and plant reproduction. *Ecotoxicology* 19:1322–1336.
4. Foy CL, Witt HL. 1990. Seed protectants safen sorghum (*Sorghum bicolor*) against chloroacetamide herbicide injury. *Weed Technol* 4:886–891.
5. DeRidder BP, Goldsbrough PB. 2006. Organ-specific expression of glutathione *S*-transferases and the efficacy of herbicide safeners in *Arabidopsis*. *Plant Physiol* 140:167–175.
6. Cui J, Zhang R, Wu GL, Zhu HM, Yang H. 2010. Salicylic acid reduces napropamide toxicity by preventing its accumulation in rapeseed (*Brassica napus* L.). *Arch Environ Contam Toxicol* 59:100–108.
7. Jiang L, Ma L, Sui Y, Han SQ, Wu ZY, Feng YX, Yang H. 2010. Effect of manure compost on the herbicide prometryne bioavailability to wheat plants. *J Hazard Mater* 184:337–344.
8. Xiao LY, Jiang L, Ning HS, Yang H. 2008. Toxic reactivity of wheat (*Triticum aestivum*) plants to herbicide isoproturon. *J Agric Food Chem* 56:4825–4831.
9. Jablonkai I, Hatzios KK. 1991. Role of glutathione and glutathione *S*-transferase in the selectivity of acetochlor in maize and wheat. *Pestic Biochem Physiol* 231:221–231.
10. Hatton PJ, Dixon D, Coleb DJ, Edwards R. 1996. Glutathione transferase activities and herbicide selectivity in maize and associated weed species. *Pesticide Science* 46:267–275.
11. Cole DJ. 1994. Detoxification and activation of agrochemicals in plants. *Pesticide Science* 42:209–222.
12. Scarponi L, Quagliarini E, Del Buono D. 2006. Induction of wheat and maize glutathione *S*-transferase by some herbicide safeners and their effect on enzyme activity against butachlor and terbuthylazine. *Pest Manag Sci* 62:927–932.
13. Dixon DP, Edwards R. 2010. Glutathione transferases. *Arabidopsis Book* 8:e0131. doi:10.1199/tab.0131.
14. Dixon DP, Cummins I, Cole DJ, Edwards R. 1998. Glutathione-mediated detoxification systems in plants. *Curr Opin Plant Biol* 1:258–266.
15. Edwards R, Dixon DP, Walbot V. 2000. Plant glutathione *S*-transferases: Enzymes with multiple functions in sickness and in health. *Trends Plant Sci* 5:193–198.
16. Marrs KA. 1996. The functions and regulation of glutathione *S*-transferases in plants. *Annu Rev Plant Physiol Plant Mol Biol* 47:127–158.
17. Cho HY, Yoo SY, Kong KH. 2006. Cloning of a rice tau class GST isozyme and characterization of its substrate specificity. *Pestic Biochem Physiol* 86:110–115.
18. Gill SS, Tuteja N. 2010. Reactive oxygen species and antioxidant machinery in abiotic stress tolerance in crop plants. *Plant Physiol Biochem* 48:909–930.
19. Faheed FA. 2012. Comparative effects of four herbicides on physiological aspects in *Triticum sativum* L. *Afr J Ecol* 50:29–42.
20. Štajner D, Popović M, Štajner M. 2003. Herbicide induced oxidative stress in lettuce, beans, pea seeds and leaves. *Biol Plant* 47:575–579.
21. Liu HJ, Xiong MY, Tian BL. 2012. Comparative phytotoxicity of Rac-metolachlor and S-metolachlor on rice seedlings. *J Environ Sci Health B* 47:410–419.
22. Dean JV, Gronwald JW, Eberlein CV. 1990. Induction of glutathione *S*-transferase isozymes in sorghum by herbicide antidotes. *Plant Physiol* 92:467–73.
23. Dayan FE, Watson SB. 2011. Plant cell membrane as a marker for light-dependent and light-independent herbicide mechanisms of action. *Pestic Biochem Physiol* 101:182–190.
24. Kopsell DA, Armel GR, Abney KR, Vargas JJ, Brosnan JT, Kopsell DE. 2011. Leaf tissue pigments and chlorophyll fluorescence parameters vary among sweet corn genotypes of differential herbicide sensitivity. *Pestic Biochem Physiol* 99:194–199.
25. Lancashire PD, Bleiholder H, Van den Boom T, Langelüddeke P, Stauss R, Weber E, Witzenberger A. 1991. A uniform decimal code for growth stages of crops and weeds. *Ann Appl Biol* 119:561–601.
26. Dhindsa R, Plumbdhinsa P, Thorpe T. 1981. Leaf senescence: Correlated with increased levels of membrane permeability and lipid peroxidation, and decreased levels of superoxide dismutase. *J Exp Bot* 32:93–101.
27. Lichtenthaler HK, Buschmann C, Knapp M. 2005. How to correctly determine the different chlorophyll fluorescence parameters and the chlorophyll fluorescence decrease ratio RFd of leaves with the PAM fluorometer. *Photosynthetica* 43:379–393.
28. Daudi A, Cheng Z, O'Brien JA, Mammarella N, Khan S, Ausubel FM, Bolwell GP. 2012. The apoplastic oxidative burst peroxidase in *Arabidopsis* is a major component of pattern-triggered immunity. *Plant Cell* 24:275–287.
29. Kerchev P, Ivanov S. 2008. Influence of extraction techniques and solvents on the antioxidant capacity of plant material. *Biotechnol Biotechnol Equip* 22:556–559.
30. McCord JM, Fridovich I. 1969. Superoxide dismutase: An enzymatic function for erythrocuprein (hemocuprein). *J Biol Chem* 244:6049–6055.
31. Bergmeyer HU, Gawenn K, Grassl M. 1974. Enzymes as biochemical reagents. In Bergmeyer HU, ed, *Methods in Enzymatic Analysis*. Academic, New York, NY, USA, pp 425–522.
32. Czaninski Y, Imberty A, Catesson A. 1984. Cytochemical-localization and parallel biochemical analysis of vegetal peroxidases. *Biol Cell* 51: A34.
33. Schröder P, Collins C. 2002. Conjugating enzymes involved in xenobiotic metabolism of organic xenobiotics in plants. *Int J Phytoremediation* 4:247–265.
34. Scalla R, Roulet A. 2002. Cloning and characterization of a glutathione *S*-transferase induced by a herbicide safener in barley (*Hordeum vulgare*). *Physiol Plant* 116:336–344.
35. Gerbling K, Kelly G, Fischer K, Latzko E. 1984. Partial purification and properties of soluble ascorbate peroxidases from pea leaves. *J Plant Physiol* 115:59–67.
36. Queval G, Noctor G. 2007. A plate reader method for the measurement of NAD, NADP, glutathione, and ascorbate in tissue extracts: Application to redox profiling during *Arabidopsis* rosette development. *Anal Biochem* 363:58–69.
37. Mamy L, Gabrielle B, Barriuso E. 2008. Measurement and modelling of glyphosate fate compared with that of herbicides replaced as a result of the introduction of glyphosate-resistant oilseed rape. *Pest Manag Sci* 64:262–275.
38. Coleman JOD, Randall R, Blake-Kalff MMA. 1997. Detoxification of xenobiotics in plant cells by glutathione conjugation and vacuolar compartmentalization: A fluorescent assay using monochlorobimane. *Plant Cell Environ* 20:449–460.
39. Jo HJ, Lee JJ, Kong KH. 2011. A plant-specific tau class glutathione *S*-transferase from *Oryza sativa* with very high activity against 1-chloro-2,4-dinitrobenzene and chloroacetanilide herbicides. *Pestic Biochem Physiol* 101:265–269.
40. Thom R, Cummins I, Dixon DP, Edwards R, Cole DJ, Lapthorn AJ. 2002. Structure of a tau class glutathione *S*-transferase from wheat active in herbicide detoxification. *Biochemistry* 41:7008–7020.
41. Viger PR, Eberlein CV, Fuerst EP, Gronwald JW. 1991. Effects of CGA-154281 and temperature on metolachlor absorption and metabolism, glutathione content, and glutathione-*S*-transferase activity in corn. *Weed Sci* 39:324–328.
42. Prior R, Wu X, Schaich K. 2005. Standarized methods for the determination of antioxidant capacity and phenolics in foods and dietary supplements. *J Agric Food Chem* 53:4290–4302.
43. Fryer MJ. 1992. The antioxidant effects of thylakoid vitamin E (alpha-tocopherol). *Plant Cell Environ* 15:381–392.
44. Munné-Bosch S. 2005. The role of α-tocopherol in plant stress tolerance. *J Plant Physiol* 162:743–748.
45. Luna CM, Gonzalez CA, Trippi VS. 1994. Oxidative damage caused by an excess of copper in oat leaves. *Plant Cell Physiol* 35:11–15.
46. Song NH, Yin XL, Chen GF, Yang H. 2007. Biological responses of wheat (*Triticum aestivum*) plants to the herbicide chlorotoluron in soils. *Chemosphere* 68:1779–1787.
47. Feierabend J, Schaan C, Hertwig B. 1992. Photoinactivation of catalase occurs under both high- and low-temperature stress conditions and accompanies photoinhibition of photosystem II. *Plant Physiol* 100:1554–1561.
48. Bestwick CS. 1998. Localized changes in peroxidase activity accompany hydrogen peroxide generation during the development of

a nonhost hypersensitive reaction in lettuce. *Plant Physiol* 118:1067–1078.
49. Lee BR, Kim KY, Jung WJ, Avice JC, Ourry A, Kim TH. 2007. Peroxidases and lignification in relation to the intensity of water-deficit stress in white clover (*Trifolium repens* L.). *J Exp Bot* 58:1271–1279.
50. Wang S, Li H, Lin C. 2013. Physiological, biochemical and growth responses of Italian ryegrass to butachlor exposure. *Pestic Biochem Physiol* 106:21–27.
51. Mittler R, Vanderauwera S, Gollery M, Van Breusegem F. 2004. Reactive oxygen gene network of plants. *Trends Plant Sci* 9:490–498.
52. Levine A, Tenhaken R, Dixon R, Lamb C. 1994. H_2O_2 from the oxidative burst orchestrates the plant hypersensitive disease resistance response. *Cell* 79:583–593.
53. Hayes JD, Pulford DJ. 1995. The glutathione *S*-transferase supergene family: Regulation of GST* and the contribution of the isoenzymes to cancer chemoprotection and drug resistance. *Crit Rev Biochem Mol Biol* 30:445–600.
54. Böger P, Matthes B, Schmalfuß J. 2000. Towards the primary target of chloroacetamides—New findings pave the way. *Pest Manag Sci*. 56:497–508.
55. Wu J, Hwang I-T, Hatzios KK. 2000. Effects of chloroacetanilide herbicides on membrane fatty acid desaturation and lipid composition in rice, maize, and sorghum. *Pestic Biochem Physiol* 66:161–169.
56. Wilkinson RE, Duncan RR, Meredith SA, Hatzios KK. 1993. Growth and physiological responses of sorghum cultivars exposed to excess H^+ and the herbicide metolachlor. *Can J Bot* 71:533–540.
57. Serra AA, Couée I, Renault D, Gouesbet G, Sulmon C. 2015. Metabolic profiling of *Lolium perenne* shows functional integration of metabolic responses to diverse subtoxic conditions of chemical stress. *J Exp Bot* 66:1801–1816.